A Statistical Study of Unusual Tracks of Tropical Cyclones near Taiwan Island

YUETING GONG

State Key Laboratory of Severe Weather, Chinese Academy of Meteorological Sciences, Beijing, and Guangdong Meteorological Observatory, Guangzhou, China

YING LI

State Key Laboratory of Severe Weather, Chinese Academy of Meteorological Sciences, Beijing, China

DA-LIN ZHANG

State Key Laboratory of Severe Weather, Chinese Academy of Meteorological Sciences, Beijing, China, and Department of Atmospheric and Oceanic Science, University of Maryland, College Park, College Park, Maryland

(Manuscript received 29 March 2017, in final form 21 October 2017)

ABSTRACT

Tropical cyclones (TCs) tend to change translation direction and speed when moving across Taiwan's Central Mountain Range (CMR), which makes forecasting of landfalling points a challenging task. This study examines the statistical characteristics of unusual TC tracks around Taiwan Island during the 66-yr period of 1949–2014. Results show that 1) about 10% more TCs were deflected to the right than to the left as they moved across the CMR, but with more occurrences of the latter on Taiwan's eastern coast and southern strait; 2) TCs around Taiwan Island moved slower than the average speed over the western North Pacific Ocean but then exhibited anomalous acceleration along Taiwan's eastern coast and anomalous deceleration over the southern Taiwan Strait; 3) about 33% of TCs passing the island were accompanied by terrain-induced secondary low pressure centers (SCs), more favored in the northwestern, southwestern, and southeastern quadrants, with the TC–SC separation distance varying from 33 to 643 km; 4) about 36% of landfalling TCs experienced discontinuous tracks, with an average separation distance of 141 km at the time when TC centers were replaced by SCs, and smaller Froude numbers than those associated with continuous-tracking TCs; and 5) a total of 12 TCs had looping movements near Taiwan Island, most of which were accompanied by SCs on their southern or western sides. Results also indicate that a stronger SC was likely to take place when a stronger TC approached the CMR with a shorter separation distance and that a weaker SC was likely to take place when a weaker TC approached the CMR with a longer separation distance.

1. Introduction

The past few decades have witnessed dramatic improvements in the forecasts of tropical-cyclone (TC) tracks because of rapid advances in computing power, numerical weather prediction models, and data assimilation and rapid growth in available remote sensing observations (Rappaport et al. 2009). As a result, 5-day TC-track forecasts have become commonplace at many national operational centers. The ability to predict unusual changes of TC movement—such as sharp turning; anomalous acceleration or deceleration; and discontinuous, looping, or rotating tracks—is very limited, however (Chen and Ding 1979; Chan et al. 1980; Carr and Elsberry 1995; Wu et al. 2013; Huang et al. 2015; Zhang et al. 2018). For example, large forecast errors occurred during the sharp northward turning of Supertyphoon Megi (2010) over the western North Pacific Ocean (WNP) (Qian et al. 2013) and during the rapid deceleration and meandering of Typhoon Morakot (2009) as it moved across Taiwan Island (Xie and Zhang 2012), both leading to unusual challenges for the issuance of effective warnings of extreme-weather conditions and subsequent disaster mitigation.

Corresponding author: Dr. Ying Li, yli@cma.gov.cn

DOI: 10.1175/JAMC-D-17-0080.1

Taiwan Island, with its Central Mountain Range (CMR) having an average elevation of 2000 m, has on average suffered from the passages of 3–4 TCs each year (Wu and Kuo 1999). Previous observational studies indicated that some westbound TCs tended to deflect southward when approaching Taiwan Island (e.g., Yeh and Elsberry 1993a; Wu 2001) and some tended to deflect northward and then move cyclonically around the northern side of the CMR (e.g., Brand and Blelloch 1974; Wang 1980). Dai et al. (2014) examined the statistical characteristics of TC tracks over the WNP during the period of 1949–2010 and showed that the frequency of right-turning TCs (55.43%) was about 10% higher than that of left-turning TCs (44.57%). The above review indicates clearly the possible effects of complex topography associated with the CMR plus the southeastern mountainous coast of mainland China and the Taiwan Strait on the unusual tracks of TCs over the WNP. Figure 1a shows three typical types of unusual TC tracks associated with Typhoons Bopha (2006), Saola (2012), and Soulik (2013) as they moved across Taiwan Island from the southwest or southeast.

Depending upon the direction, intensity, and static stability of incoming larger-scale flow, the CMR could alter it to parallel or splitting flows, or a blocking flow (Shieh et al. 1998), thereby influencing TC movement. The channeling effect of the Taiwan Strait tends to push TCs southward, as indicated by idealized numerical experiments in Yeh and Elsberry (1993a). Some other studies indicated that the channeling effect could make TC circulations asymmetric, leading to a southward deflection (Wu et al. 2015) and even a looping movement (Jian and Wu 2008; Huang et al. 2011). Chang (1982) stressed the importance of asymmetric diabatic heating in the eyewall in deflecting TC tracks over Taiwan Island. This result was later confirmed by Wang et al. (2013) and Hsu et al. (2013), whose studies showed that asymmetric diabatic heating plays a critical role in altering TC track, intensity, and propagation speed over the Taiwan region. Figure 1a shows two examples of unusual tracks that were mainly influenced by the CMR: Typhoon Soulik (2013) turned cyclonically around the northern side of the CMR and made a sharp northeastward deflection when moving into Taiwan Strait, and Typhoon Saola (2012) took a loop over the northeast part of Taiwan Island prior to its landfall.

Another phenomenon caused by the CMR blocking is the generation of secondary low pressure centers [also referred to as secondary cyclonic vortices (SCs)] when a TC passes over Taiwan Island. The TC track may become discontinuous when an SC develops on the lee side, and then it replaces the original TC low pressure center that is blocked on the upstream side of the CMR (Wang 1954). Typhoon Bopha (2006) is a good example of a discontinuous track (Fig. 1a), with an SC that developed to the southwest of the CMR and eventually replaced the TC center as it moved west over the sea area east of Taiwan. Numerous studies have discussed possible processes leading to such discontinuity of TC tracks. After analyzing the surface maps of 53 typhoons that passed through Taiwan and nearby regions from 1946 to 1975, Wang (1980) found that the tracks of westbound TCs approaching the CMR with weak intensity and an intercepting angle of larger than 120° would become discontinuous. Numerical model simulations of Yeh and Elsberry (1993b) showed that a TC with weaker intensity, slower translation speed, and more southern location relative to the CMR tends to have a discontinuous track, which is consistent with the observational analysis of Wang (1980).

In a series of theoretical and modeling studies, Lin et al. (2002, 2005) identified six nondimensional control parameters that determined the continuity and deflection of 16 TCs from previous observational analyses and real-case simulations. Using the maximum wind of a TC V_{MAX}, large-scale mean flow U, the radius R of V_{MAX}, the Brunt–Väisälä frequency N, the Coriolis parameter f, and the height H, half-width L_X, and length L_Y of the CMR, they found that a TC track would become discontinuous and experience likely deflection with a combination of small values of the vortex Froude number F_R $[=V_{\mathrm{MAX}}/(NH)]$, Eulerian Rossby number R_E $[=U/(fL_X)]$, and Lagrangian Rossby number R_L $[=V_{\mathrm{MAX}}/(fR)]$ and large values of the steepness of the CMR (H/L_X). In particular, $F_R = 1.5$ can be used to discern discontinuous tracks from continuous tracks, according to their studies. Peng et al. (2012) examined 121 westbound cross-Taiwan TCs between 1897 and 2009 in an attempt to identify some other variables that might be most influential to the TC track continuity, and they found that the track continuity depended mostly upon the location of landfall (YLF), the approaching direction (DIR), and V_{MAX} of a TC. Their study showed that the majority of TC tracks were discontinuous when the YLF was at Taiwan's eastern central coast and were continuous at its northern and southern regions. In particular, TC tracks would most likely be continuous when hitting the CMR at a near–right angle and would most likely be discontinuous when associated with sharp angles. Moreover, $V_{\mathrm{MAX}} = 40\,\mathrm{m\,s^{-1}}$ is an optimal speed for separating continuous from the discontinuous tracks. A logistic regression model in terms of YLF, DIR, and V_{MAX} was then developed that predicts reasonably well the continuity or discontinuity of TC tracks across Taiwan Island. Lin and Savage (2011) and Lin et al. (2016) showed through a series of idealized numerical experiments

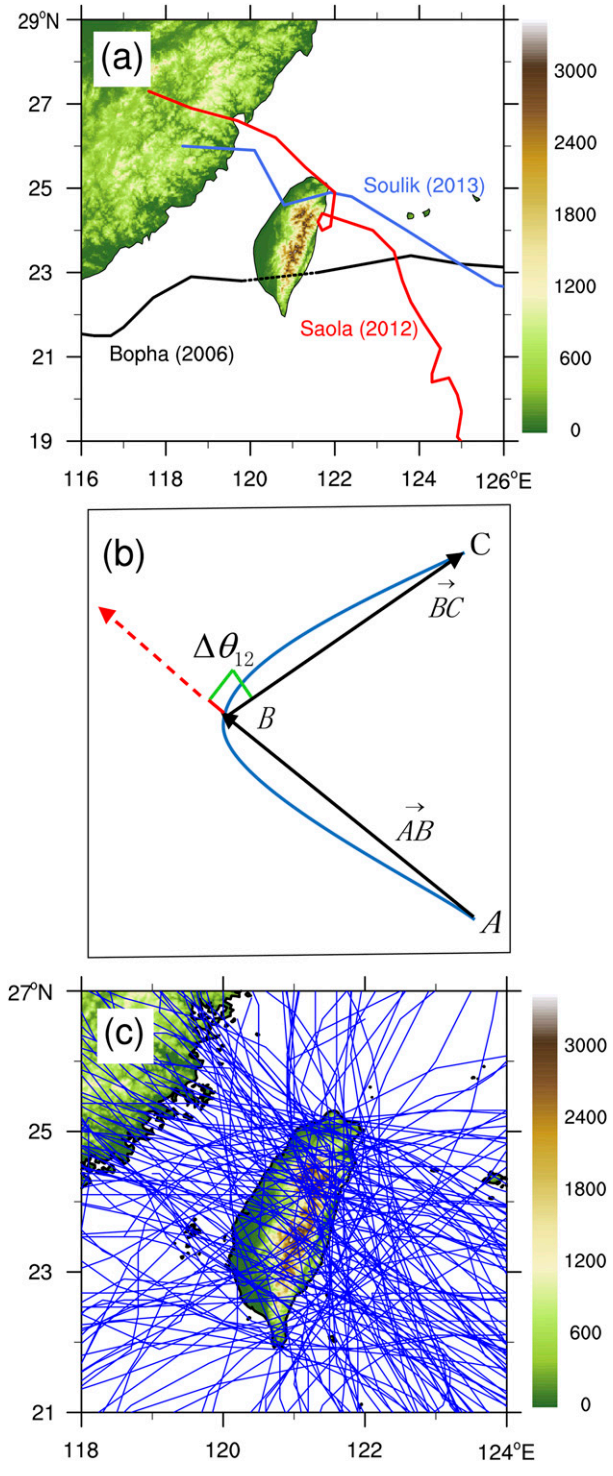

FIG. 1. (a) Samples of three different anomalous TC tracks near Taiwan Island: a discontinuous track (with dotted lines connecting TC and SC centers) of Typhoon Bopha (1960) in black, a looping track of Typhoon Saola (2012) in red, and a sharp turning track of Typhoon Soulik (2013) in blue. (b) A sketch of TC track deflection: **AB** and **BC** are the translation vectors at time $T - 6$ and $T + 6$ h, respectively, and $\Delta\theta_{12}$ is the deflection angle at point B (see the text for more detail). (c) Track segments for 121 landfalling TCs on Taiwan Island during the 66-yr period of 1949–2014. Terrain height in meters is indicated by the shading in (a) and (c).

that the degree of orographic blocking is determined mainly by the landfalling location and DIR of TCs when encountering a mesoscale mountain range and that strong orographic blocking usually results in significant deflection of TC tracks.

Numerous studies have examined some unusual movements of TCs as they move around Taiwan Island, but little attention has been paid to the formation of SCs associated with eastbound TCs and their tracking characteristics. It is also unclear how the SCs are statistically distributed around Taiwan Island and how they are related to unusual TC tracks. Thus, the major objectives of this study are 1) to explore the statistical track characteristics of TCs, including anomalous changes in both translation speed and direction, as they move across Taiwan Island and 2) to examine the statistical distribution of SCs and their relationship with the anomalous TC movements. The objectives will be achieved by analyzing the best-track data of TCs occurring over the WNP during the 66-yr period of 1949–2014.

The next section describes the data source and method employed in this study. Section 3 presents the statistical characteristics of TC motion and anomalous changes near Taiwan Island. Section 4 discusses the relationship between SCs and anomalous TC tracks. A summary and concluding remarks are given in the final section.

2. Data source and method

A TC may be regarded as a symmetric vortex covering an area with a radius of 400–1000 km (Chen and Ding 1979). The effects of Taiwan Island on TC movement may be expanded outward to about 400 km (Yeh and Elsberry 1993a; Luo and Chen 1995). Thus, an area of 116°–126°E and 19°–29°N (i.e., a 10° × 10° grid box centered on Taiwan Island) is used as a target region for this study. A TC will be treated as a sample of interest when its center falls into this area. The best tracks of TCs during the period of 1949–2014, archived at the Joint Typhoon Warning Center (JTWC; https://metoc.ndbc.noaa.gov/web/guest/jtwc/best_tracks/western-pacific), are used herein and include information on position, V_{MAX}, and the minimum sea level pressure P_{MIN} at 6-h intervals. The TC samples used herein include tropical storm (TS), severe tropical storm (STS), typhoon (TY), severe typhoon (STY), and supertyphoon (Super TY) but exclude tropical depression (TD).

Previous studies have discussed TC anomalous track deflection with different criteria, for example, 20° deflection in 12 h (Chan et al. 1980), 45° right turning in 36 h (Hodanish and Gray 1993), and 60° deflection in 24 h (Wu et al. 2011). For the operational track forecasts of TCs in China, 45° right deflection and 30° left deflection of TCs in 12 h have been used as the threshold values for anomalous track deflection angles. After examining various criteria used for anomalous track deflection over the WNP, Dai et al. (2014) provided the rationale for the above criteria, showing that the occurrence probability in 12 h of a right deflection of larger than 45° is less than 2.8% and that of a left deflection of larger than 30° is less than 8.7%. Here, a track deflection angle at a 12-h interval $\Delta\theta_{12}$ is calculated (see Fig. 1b), following Chan et al. (1980), given by

$$\Delta\theta_{12} = \arccos[\mathbf{AB} \cdot \mathbf{BC}/(|\mathbf{AB}||\mathbf{BC}|)], \quad (1)$$

where the letters A, B, and C denote the consecutive positions of TC centers at 6-h intervals (Fig. 1b). So, **AB** and **BC** represent the translation vectors at time $T - 6$ h and $T + 6$ h, respectively. A right or left deflection at time T is defined as a TC motion vector rotating clockwise (denoted as $\Delta\theta_{12} > 0$) or counterclockwise (denoted as $\Delta\theta_{12} < 0$), respectively, from the prior 6 h to the next 6 h (i.e., $T + 6$ h). A 0° value of $\Delta\theta_{12}$ implies stagnation or straight movement of the TC.

In this study, events of anomalous acceleration and deceleration are defined as a 6-h changing rate in translation speed v at time $T + 6$ h doubling or halving that at time T, respectively. A 6-h v for the period from T to $T + 6$ h is given by

$$v = R \times \arccos[\cos\omega_1 \cos\omega_2 \cos(\phi_1 - \phi_2) + \sin\omega_1\omega_2]/6, \quad (2)$$

where R (=6371 km) is Earth's mean radius and ϕ_1, ω_1 and ϕ_2, ω_2 denote the longitude and latitude of the TC center at times T and $T + 6$ h, respectively.

In addition, TC tracks at 1-h intervals are positioned according to hourly synoptic charts made by mesoscale analyses of surface observations in the Taiwan area from the Central Weather Bureau (CWB) Typhoon Data Base (http://rdc11.cwb.gov.tw/TDB/). The hourly data are used to determine 1) whether a TC track was discontinuous, 2) whether it made a loop when moving around Taiwan Island, and 3) whether an SC was formed (Shieh et al. 1998). An SC is assumed to begin when a closed isobar of depression appears on a synoptic chart near Taiwan Island andis sustained for at least 6 h. An SC center is defined by a cyclonic circulation center, and the innermost closed isobar, plotted at 2-hPa intervals, is taken as its intensity. The "best track" data of the SCs so obtained are then created to match those of the corresponding TCs during their coexisting periods.

3. Statistical characteristics of TC movements near Taiwan Island

In this section, we provide an objective analysis of the statistical characteristics of changes in TC movements (i.e., both direction and speed) in the context of annual and monthly variations and geographical distributions as well as anomalous TC movements in the vicinity of Taiwan Island.

a. Temporal variations

During 1949–2014, a total of 530 TCs occurred over the target area, in which 121 TCs (i.e., 23% of the total) made landfall on Taiwan Island (Fig. 1c) and contributed 3908 samples of 12-h track deflections. Figure 2a shows significant interannual variation of the annual frequency of TCs, with lower frequencies in the 1950s [and the lowest one (three TCs) in 1955] and higher frequencies from the 1960s to the 2010s [and the highest (14 TCs) in 1966]. The monthly mean frequency of TCs occurring over the target area varied from none in the months of January–March to a maximum of three in August, followed by a decrease from September to December (not shown), which is similar to the monthly mean TC deflection frequency shown in Fig. 2b.

b. Deflection statistics

An analysis of the 3908 samples indicates a mean directional change of 15.6° as the TCs move around Taiwan Island, which was slightly larger than the climatological mean of 14.51° for the WNP cases (Dai et al. 2014). Frequencies of the right and left deflections accounted for 51.4% and 41.3% of the total, respectively, indicating 1) that most TCs experienced directional changes and 2) that right deflections were 10% more common than left deflections during their passages over the target area. Note that 7.3% of TCs maintained their original moving directions in the next 6-h period or stagnated. Figure 2b shows that the monthly deflection frequency varied similarly to the monthly frequency of TCs over the target area, with slightly higher right-deflecting frequencies than left-deflecting frequencies except in the month of August. The deflection frequency as a function of deflection angle, as given in Fig. 2c, shows that it decreased with deflection angle from 0° to 90° but increased when the deflection angle was greater than 90°; these large deflection angles are mainly contributed by looping and rotating samples.

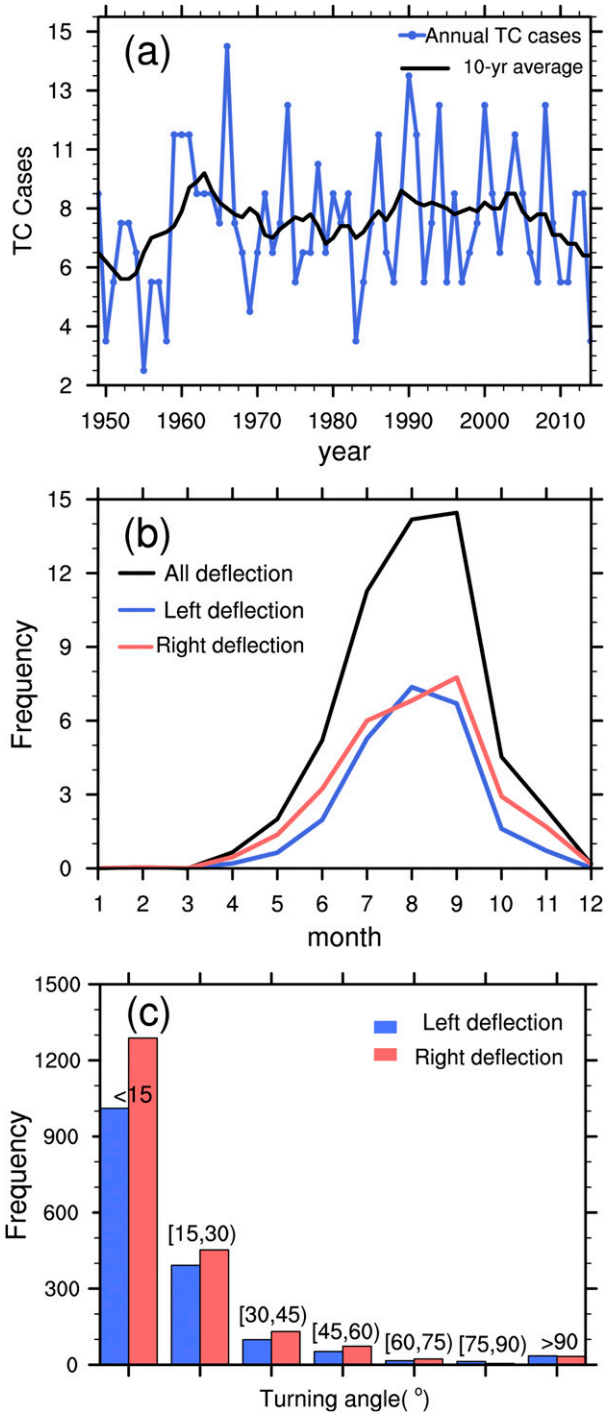

FIG. 2. (a) Time series of the annual frequencies of TCs occurring near Taiwan Island (blue) and their 10-yr running average (black) during the 66-yr period of 1949–2014. (b) Monthly variation of the TC deflection frequencies for all TCs (black) and for the left (blue) and right (red) deflections. (c) Angular variation of the left and right deflection frequencies with deflection angle, at 15° intervals.

c. *Geographical distribution of directional and speed changes around Taiwan Island*

The accumulated frequency distribution of TC deflection on a 0.5° × 0.5° grid (Fig. 3a) indicates that track deflection was spatially inhomogeneous around Taiwan Island. A large number of deflection samples (i.e., ~80%) occurred over the area to the south of 25°N where TC passage frequency was high. It is clear that higher deflection frequencies were observed in the northern portion and the eastern coastal region of Taiwan Island as well as the Taiwan Strait. Left-deflecting TCs appeared more often than right-deflecting ones over the eastern coast of Taiwan Island and the southern portion of the Taiwan Strait, whereas the opposite was true over the western coast of Taiwan Island and especially the northwestern coastal area (Fig. 3b). Many impact factors have been proposed to explain the track deflection, including larger-scale cyclonic circulation (Bender et al. 1987), advection by topographically blocked flows (e.g., Yeh and Elsberry 1993a,b), asymmetric latent heat release (e.g., Chan et al. 2002; Hsu et al. 2013; Wang et al. 2013; Tang and Chan 2014, 2015), and northerly asymmetric latent heating effect (Wu et al. 2015). Lin et al. (2016) examined the above impact factors through a series of idealized numerical experiments and found that orographically blocked flows and asymmetric latent heat release play more important roles in determining upstream track deflection.

The averaged TC translation speed in the next 6 h over the target area was 17.5 km h^{-1}, which was slower than that of the WNP, which averaged 21.6 km h^{-1} (Dai et al. 2014). The TC translation speeds on a 0.5° × 0.5° grid, given in Fig. 3c, show that faster speeds were observed over southern Taiwan and its eastern coast and slower speeds were found over the southern Taiwan Strait and northern Taiwan. An analysis of the TC moving speeds from time T to $T + 6$ h and $\Delta\theta_{12}$ from time $T - 6$ h to $T + 6$ h, given in Fig. 3d, reveals that a majority of TCs moved at speeds of less than 30 km h^{-1} with deflection angles of less than 30°. It is also seen, however, that a significant number of faster- and slower-moving TCs had deflection angles of less than and more than 30°, respectively. The different correlations between moving speeds and deflection angles might be determined by different values of F_R, R_E, and R_L, on the basis of the previous studies mentioned in section 1.

d. *Anomalous movements*

It is well known that a TC may undergo anomalous changes in both moving direction and translation speed. As mentioned in section 2, previous studies have examined TC anomalous track deflection with different

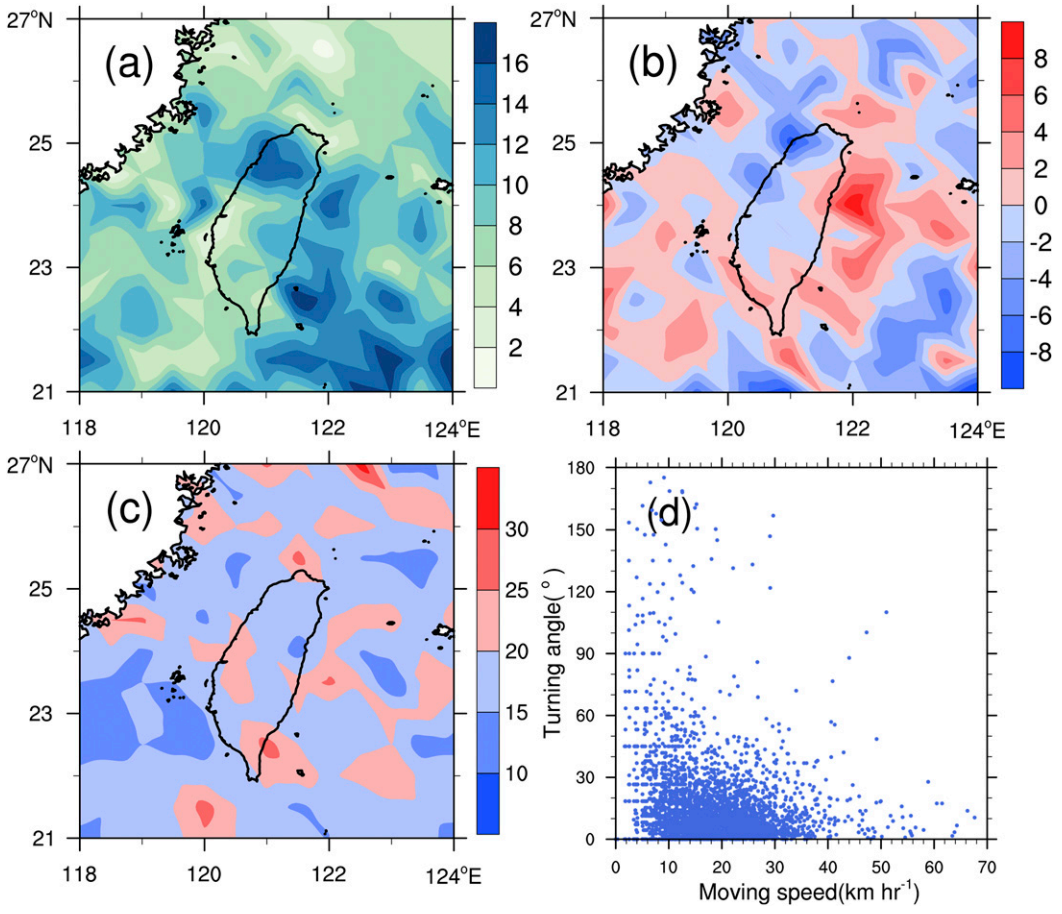

FIG. 3. The geographical distribution of (a) accumulated TC deflection frequency (%; shading), (b) accumulated deflection frequency differences (%; shading) between left- and right-turning TCs, (c) averaged 6-h moving speed v (km h^{-1}; shading), and (d) absolute values of $\Delta\theta_{12}$ (°) as a function of v during the 66-yr period of 1949–2014.

criteria, for example, varying from 20° deflection in 12 h to 45° right turning in 36 h, and 60° deflection over 24 h, and the operational track forecasts of TCs in China use 45° right deflection and 30° left deflection in 12 h as the threshold values for anomalous track deflection angles. To facilitate comparison with their results, the same criterion as the above operationally used one is adopted herein to screen anomalous deflecting events. Results show that 349 anomalous deflecting events occurred in the Taiwan region during the period of 1949–2014, which accounted for 8.9% of the total samples. Among them, 3.5% were right turning and 5.4% were left turning, reflecting a higher likelihood for TCs to experience left deflection anomaly. These results are consistent with those of Dai et al. (2014) that anomalous changes in TC moving direction were generally of small probability but that the probability of anomalous right (left) turnings over Taiwan area is higher (lower) than that over the WNP (2.74% for right anomalous turning and 8.69% for left anomalous turning). Figure 4a displays the percentage of anomalous deflections in each 0.5° × 0.5° grid box, showing that a relatively higher proportion of areas (reaching 40%) of anomalous deflection appeared over the northeastern coast of Taiwan Island and southern Taiwan Strait with 95% statistical significance.

The proportion of anomalous translation speed is given in Fig. 4b, showing that TCs landfalling on the eastern side of Taiwan Island and those moving into the southern Taiwan Strait were more likely to experience anomalous translation speeds with a higher proportion of 10%–30% at 95% statistical significance. The former tended to accelerate as a result of significant changes in moving speeds of looping or rotating TCs prior to landfall, whereas the latter were likely to decelerate because of the feedback from asymmetric rainfall and diabatic heating induced by mesoscale topography of Taiwan (Wang et al. 2013). The existence of the CMR could also affect TC translation through upstream blocking and/or downstream acceleration.

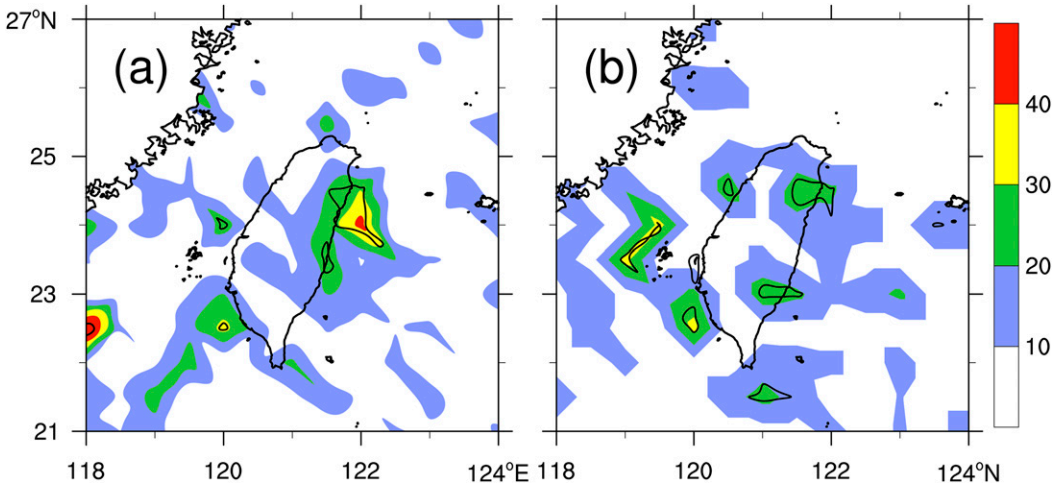

FIG. 4. (a) Proportion of anomalous track deflection (%; shading) in each 0.5° × 0.5° grid box with respect to the total track deflections during the 66-yr period of 1949–2014, with black contours indicating areas passing 95% significance. (b) As in (a), but for the anomalous changes of translation speeds.

A comparison of Figs. 4 and 3a reveals that, although the mean frequency of TCs moving across Taiwan Island was much smaller than that in the Southern Ocean, the probability of anomalous movements in the vicinity of Taiwan Island was significantly higher than that in the Southern Ocean. This result indicates clearly the important role of topography in determining the changes in TC movements, which motivates us to examine in the next section what and how topography alters the movement of TCs.

4. Relationship between TC movement and the formation of SCs

In this section, the impact of the CMR on TC movements is explored by analyzing the statistical characteristics of topographically generated SCs near Taiwan Island, including the life spans, intensities, and geographical distributions of TCs accompanying the SCs. In addition, the relationship between the two related systems is examined in terms of intensity, separation distance, and relative movement as well as anomalous movement (e.g., discontinuous, and looping tracks).

a. Statistical characteristics of SCs

Previous studies have shown that topographically generated SCs could change TC displacements to some degree, sometimes causing sharp deflection of TC tracks (Meng et al. 1998) or discontinuous TC tracks (Shieh et al. 1998). Before studying the relationship between the formation of SCs and changes in TC movement, it is desirable to examine first the spatial characteristics of SCs using hourly synoptic surface charts from the CWB's Typhoon Data Base.

An analysis of the CWB's data reveals that about 33% (i.e., 175 TCs) of the total (530 TCs) were found to coexist with SCs in the target area, 45% (i.e., 79 TCs) of which made landfall on Taiwan Island. In addition, we have identified 245 SCs, with a total of 599 samples at 6-h intervals, that coexisted with TCs occurring in the vicinity of Taiwan Island, implying that more than one SC has occurred during the passage of a TC. In fact, TCs coexisting with one and two SCs accounted for 63% and 34% of the 175 TCs, respectively. We have even found four TCs coexisting with three SCs each (e.g., Typhoon Nakri of 2002), and one TC coexisting with four SCs (i.e., Typhoon Virginia of 1957) from the CWB's Typhoon Data Base.

Although the SC life spans varied from case to case, we find that SCs with a 12-h life span accounted for 35% of the total, followed by 28% and 21% with 18- and 6-h life spans, respectively. The longest life span of an SC was about 54 h along the eastern coast of Taiwan Island when Typhoon Nari (2001) moved slowly along the CMR's western foothills from the northeast to southwest (Yang et al. 2008, 2011). In general, SC intensities varied from 964 to 1008 hPa, with a mean value of 994 hPa, and 75% were deeper than 1000 hPa (Fig. 5a). Detailed intensity stratifications are given ncxt in section 4b.

b. Intensity stratification of TCs and SCs and their separation distances

After seeing the statistical significance of the topographically induced SCs accompanied by TCs, it is of interest to examine the formation of SCs in relation to the intensities of TCs (Fig. 5b) and their separation distances (Fig. 5c). The TC intensity is represented

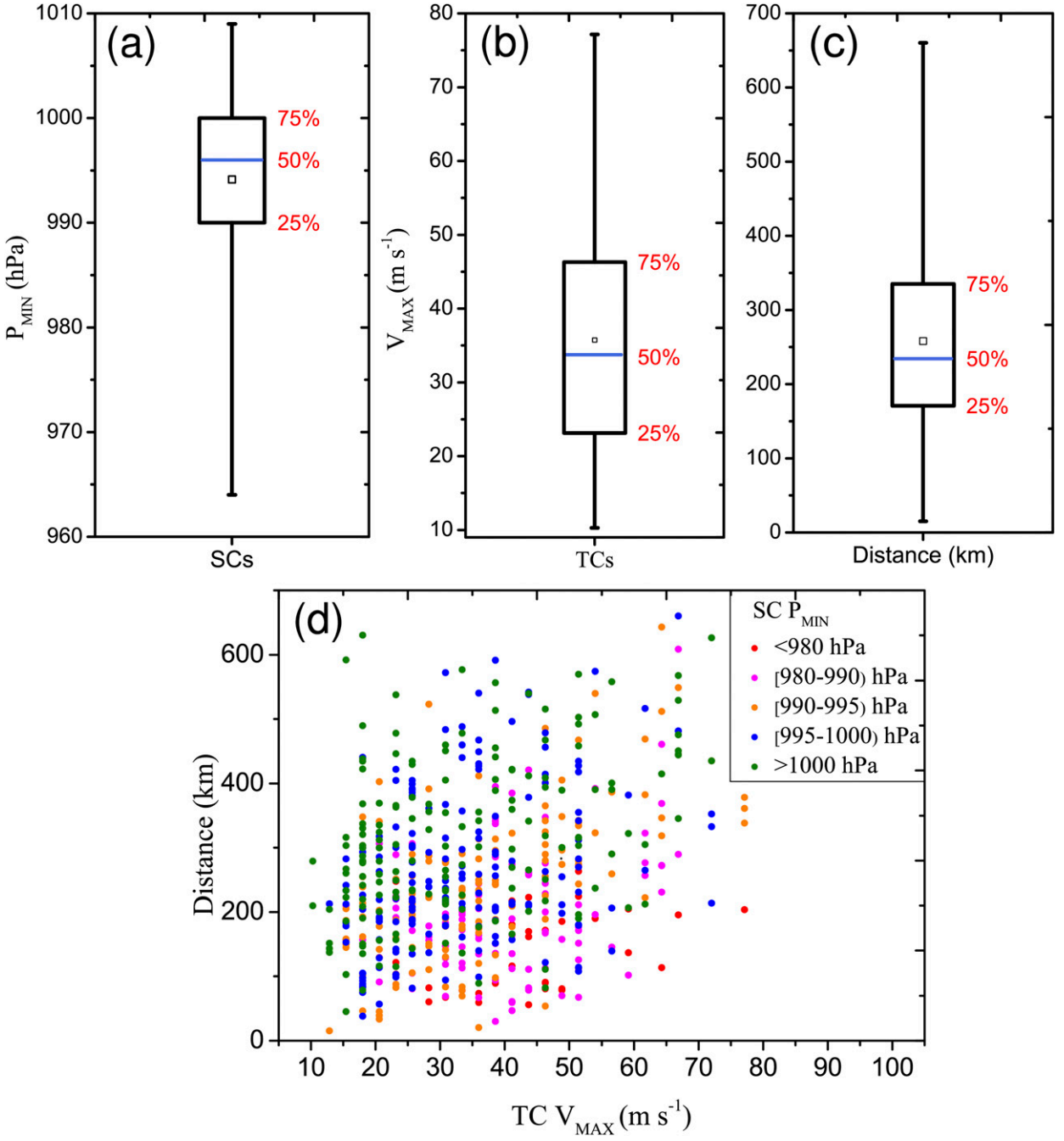

FIG. 5. Box-and-whisker plots of (a) P_{MIN} (hPa) of SCs, (b) V_{MAX} ($m\,s^{-1}$) of TCs coexisting with SCs, and (c) their separate distances (km) during the 66-yr period of 1949–2014. Boxes show interquartile ranges; whiskers show the first quartile and the fourth quartile. The top and bottom horizontal bars denote the maximum and minimum values. The blue bar denotes the median value, and the open square denotes the average value. (d) The separation distance between TCs and SCs as a function of TC intensity under five intensity categories of SCs.

herein by only V_{MAX} because of the absence of P_{MIN} records in the JTWC dataset prior to 2001. Figure 5b shows that V_{MAX} ranged from 10 to 77 $m\,s^{-1}$, implying that any TC with an intensity category from TD to Super TY could induce an SC, with most in the categories from STS to STY. The average TC intensity was 36 $m\,s^{-1}$ reaching a TY category; nevertheless, STSs tended to induce more SCs in total than TCs in the other categories, that is, they accounted for 26% of the total SCs. Note that, although TDs were excluded from our TC

database, about 5% of the TCs coexisting with SCs occurred at their TD stage.

The separation distances between TCs and SCs were found to range from 33 to 643 km, with an average distance of 259 km; the shortest and longest distances were associated with Typhoons Jangmi (2009) and Sally (1964), respectively (not shown). The separation distances of larger than 400 km may be attributed partly to some SCs that were formed under the influences of other weather systems around Taiwan Island during TCs' passages and partly to some SCs that developed without replacing the TCs' centers after they moved away.

The intensity of SCs can be stratified into five categories: lower than 980 hPa, 980–990 hPa, 990–995 hPa, 995–1000 hPa, and higher than 1000 hPa, giving 34, 98, 133, 170, and 164 samples, respectively. Figure 5d shows the TC–SC separation distance as a function of TC intensity in V_{MAX} under the five intensity categories of SCs. Results indicate that, for a given TC intensity, the smaller the separation distance was, the stronger was the SC that tended to form. In a similar way, for a given separation distance, the stronger a TC was, the more intense was the SC that tended to form. Thus, we may state that the intensity of an induced SC was closely related to TC intensity and their separation distance. In other words, when a stronger TC moved closer to Taiwan Island, its interaction with the CMR was larger and therefore a stronger SC would be induced, and when a weaker TC moved closer to Taiwan Island, its interaction with the CMR was smaller and therefore a weaker SC would be induced.

c. *Distribution of TCs and associated SCs in different quadrants*

Figure 6a shows the geographical distribution of SCs, occurring mostly on both sides of the CMR, but more favorably in the western quadrants and southeastern quadrant if the CMR ridge is used as a "longitude" axis. A few of them even occurred to the north of 28°N over the East China Sea (not shown). Most SCs remained stagnant after their formation and then dissipated, whereas some of the other ones migrated northward to replace their corresponding original TC centers, resulting in discontinuous tracks.

To display the relative positions between TCs and SCs, the target domain is separated into four parts as northeastern (NE), northwestern (NW), southwestern (SW), and southeastern (SE) quadrants by two lines perpendicular to each other at the point 23.5°N, 121°E on the along-ridge axis of the CMR (see Fig. 6a). The locations of TC centers (red dots) and coexisting SC centers (blue open triangles) in the above four quadrants are shown in Figs. 6b–e, respectively. Although the NE quadrant had the least number of SCs (only 6.5% of the total; Fig. 6b), the average intensity of SCs reached 992 hPa, which was the strongest one among the four quadrants. The corresponding TCs were mainly located to the west of the SCs covering the Taiwan Strait, with a small portion of their positions overlapped with SC positions and a few of them located to the northeast of the SCs. In contrast, the NW quadrant had the largest number of SCs (about 38% of the total; Fig. 6c), with the weakest mean intensity of 996 hPa. Most of the corresponding TCs were dispersed over a wide area to the south of the SCs, including the Taiwan Strait, Taiwan Island, and the surrounding sea area. The most remote TCs occurred to the south of 19°N (not shown). Only a few TCs were located farther north of SC positions. About 27% of the total SCs were located in the SW quadrant (Fig. 6d), with an average intensity of 994 hPa. Most of the corresponding TCs were located to the east and south of the SCs, with a few to the west and north of the SCs. The SE quadrant contained 28.5% of the total SCs (Fig. 6e), with an average intensity of 993 hPa, which is similar in both percentage and SC intensity to those in the SW quadrant (cf. Figs. 6d and 6e). The corresponding TCs were primarily located on the north and west sides of the SCs, covering Taiwan Island, the Taiwan Strait, and the northern sea area up to approximately 28°N.

The above analysis of the relative positions of TCs and SCs indicates that the interaction of TCs in different orientations with the CMR could induce SCs over different areas around Taiwan Island. Most of the TCs and SCs were located on the opposite sides of the elongated CMR. That is, TCs moving over the east side of the CMR tended to induce SCs on the west side of the CMR, and those moving over west side of the CMR tended to induce SCs on the east side of the CMR, with only with a small portion of them occurring on the same side.

d. *Relative movements between TCs and SCs*

Once an SC forms over the Taiwan area, it may either move away or remain there during the passage of the corresponding TC. In doing so, a relative motion between the TC and SC may occur. With the best-track data of TCs and SCs, the relative motions of TCs and SCs are represented by 6-h angular changes of the orientation of a straight line connecting the two vortex centers. A cyclonic rotation of the line is defined as positive, and an anticyclonic rotation is defined as negative.

There were 173 TCs accompanied by 245 SCs during the 66-yr period of 1949–2014, which gave a total of 358 6-h periods. An analysis of the data indicates that cyclonic and anticyclonic rotations accounted for 188 (~53%) and 170 (~47%), respectively; only one case

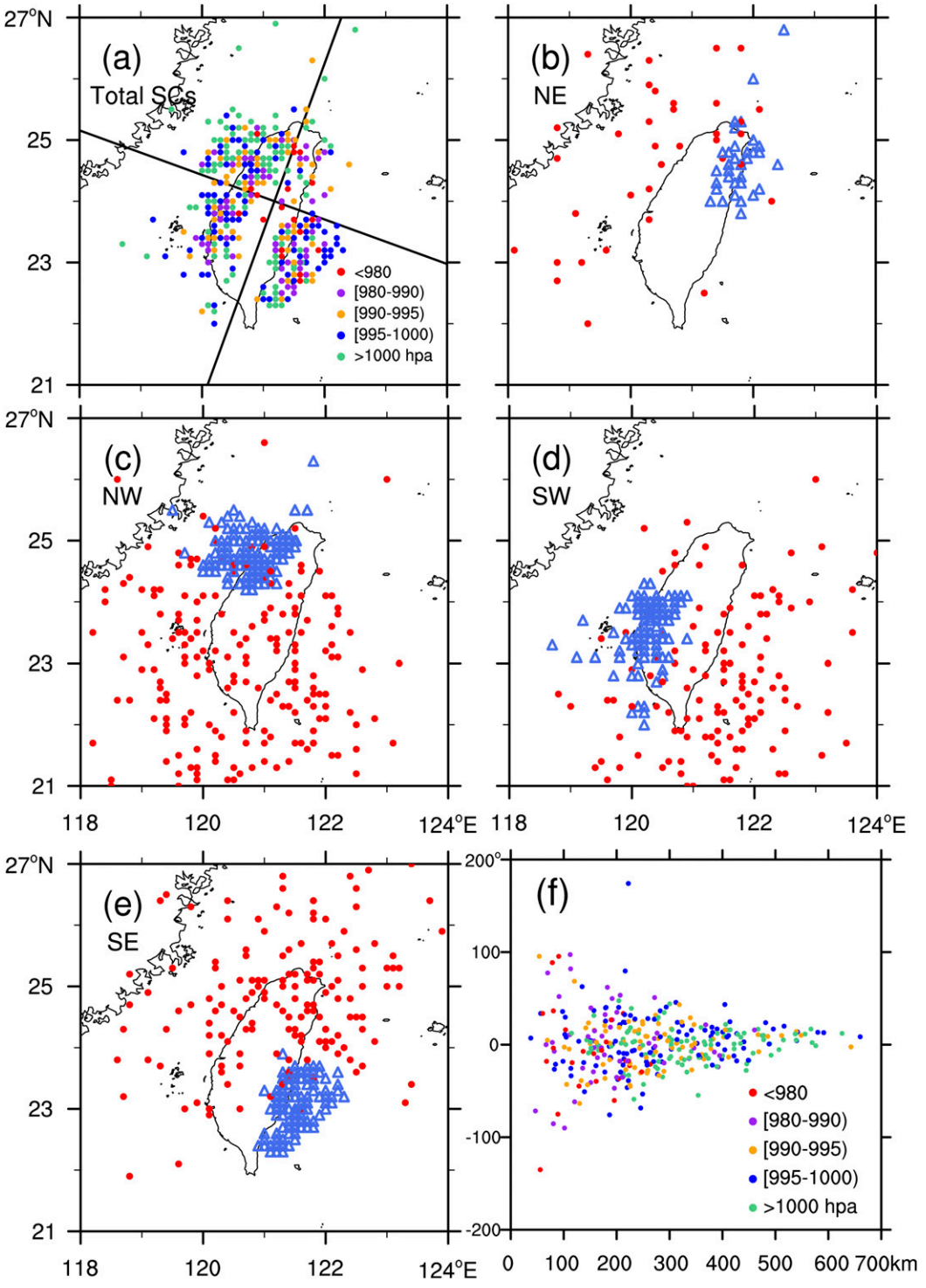

FIG. 6. (a) Horizontal distribution of the total SCs induced by TCs passing by Taiwan Island during the 66-yr period of 1949–2014. Also shown are the relative positions of SCs (blue open triangles) and their coexisting TCs (red dots) in the (b) NE, (c) NW, (d) SW, and (e) SE quadrants. (f) Rotation angles of the relative movements between TCs and SCs as a function of separation distance for SCs under different intensity categories (see text).

occurred without a notable angular change. Among the 358 samples, 121 (34%) TC centers were accompanied by SC centers on the south side and 237 (66%) TC centers were accompanied by SC centers on the north side. In the former, cyclonic rotations accounted for a higher proportion of about 78% with the mean angular change of 15.5°, whereas, in the latter, anticyclonic rotations accounted for 68% of the total with a mean angular change of −8.5°. Figure 6f shows the 6-h angular changes in relative movement as a function of separation distance in different categories of SC intensity. Results indicate that the shorter the separation distance was and the stronger the SC was, the more significant was the angular change for both the cyclonic and anticyclonic rotations. When the separation distance was shorter than 100 km, the angular changes increased sharply to 100°. On the other hand, when the distance increased to more than 500 km, little angular change was observed. These phenomena could be understood as follows: Given the fact that most SCs did not exhibit significant displacements relative to their counterparts, the angular changes would be more pronounced when a TC moved closer to Taiwan Island, unless an SC was formed right at the front in the TC path.

e. *Discontinuous tracks of TCs in relation to SCs*

A TC's track is regarded as being discontinuous when it passes over Taiwan Island with an accompanying SC that develops and later replaces the original TC center. During the 66-yr study period, 36% of the landfalling TCs (44 cases) experienced discontinuous tracks. Figures 7a and 7b show the relative locations of TCs and SCs at the time prior to their center replacements during the 66-yr period of 1949–2014. It is evident that most discontinuous tracks were associated with TCs that crossed Taiwan westbound (Fig. 7a), which were replaced by SCs on the west side of the CMR. Only six TCs that crossed Taiwan eastbound experienced discontinuous tracks (Fig. 7b), three of which were replaced by SCs on the east side of the CMR and the remaining three of which were replaced by SCs on the same west side. The separate distances between the TC and SC centers were calculated for the discontinuous track samples. Results indicate that the average distance varied from 59 to 249 km with a mean value of 141 km, which was shorter than that of all of the TCs and associated SCs. The average intensity of such SCs was 991 hPa, which was 3 hPa stronger than that of all of the SCs during the 66-yr study period.

As mentioned in section 1, Lin et al. (2002, 2005) indicated that the TC vortex Froude number F_R can discern discontinuous from continuous tracks. In this study, we estimated F_R for all landfalling TCs, following their studies using V_{MAX} from the best-track data, N calculated over the area of a 5° × 5° grid box centered at the TC center using the National Centers for Environmental Prediction reanalysis on a 2.5° × 2.5° grid at 6 h prior to landfall on Taiwan, and H = 2.5 km as the average height of the CMR. Results show that most F_R values for discontinuous tracks occur in the range of 1.3–1.8, with an average of 1.57, which is smaller than continuous tracks with a range of 1.5–2.3, with an average of 1.91. Prior to landfall, the average TC intensity with discontinuous tracks is 38.4 m s^{-1}, which was weaker than that of TCs with continuous tracks (~44.7 m s^{-1}). These results are consistent with those of Lin et al. (2002, 2005), who found that a weaker TC with a smaller F_R value tended to have a discontinuous track. This result means that it is more difficult for a weaker vortex with a more stable stratification to pass over the CMR; it likely will pass around it so that its center is more likely to be replaced by its associated SC on the lee side. Rostom and Lin (2015) recently extended the study of Lin et al. (2005) to extratropical cyclones over the Appalachian Mountains and indicated that discontinuous tracks occur when $F_R < 1.5$ and $R_L < 4.0$ are both true. Results from our 2001–14 samples show that the mean R_L value of discontinuous tracks is 2.6, with 75% of them having $R_L < 3.7$, which is in agreement with the work of Rostom and Lin (2015).

f. *Looping tracks of TCs in relation to SCs*

A TC may make a looping track when it is blocked by the CMR, such as was the case for Typhoons Haitang (2005), Krosa (2007), and Saola (2012). A TC interacting with an SC can also make a looping track, however, according to the study of Yang et al. (2011). Our analysis of the 66-yr best-track data reveals that a total of 12 TCs (~2.3%) experienced cyclonic looping movement over northern Taiwan Island and its northeastern coastal water. During the course of looping movements, 11 of the 12 TCs were accompanied by SCs: 9 of them had SCs on the southern side and the remaining 2 had SCs on the western side (Fig. 7c). After analyzing the 12 looping tracks, an area covering all their positions at 6-h intervals is determined as a possible area for looping TC tracks, which is given as an inner box in Figs. 7c,d. However, our analyses indicate that another 101 TCs went through this possible area without looping movements during the 66-yr study period. About 73% of them had accompanying SCs regardless of the relative orientation between the two systems. Only 36% of them were accompanied by SCs on their southern side (Fig. 7d), which was much less than the percentage of the looping TCs. It follows that looping TCs would more likely induce SCs on their southern side, thereby influencing in

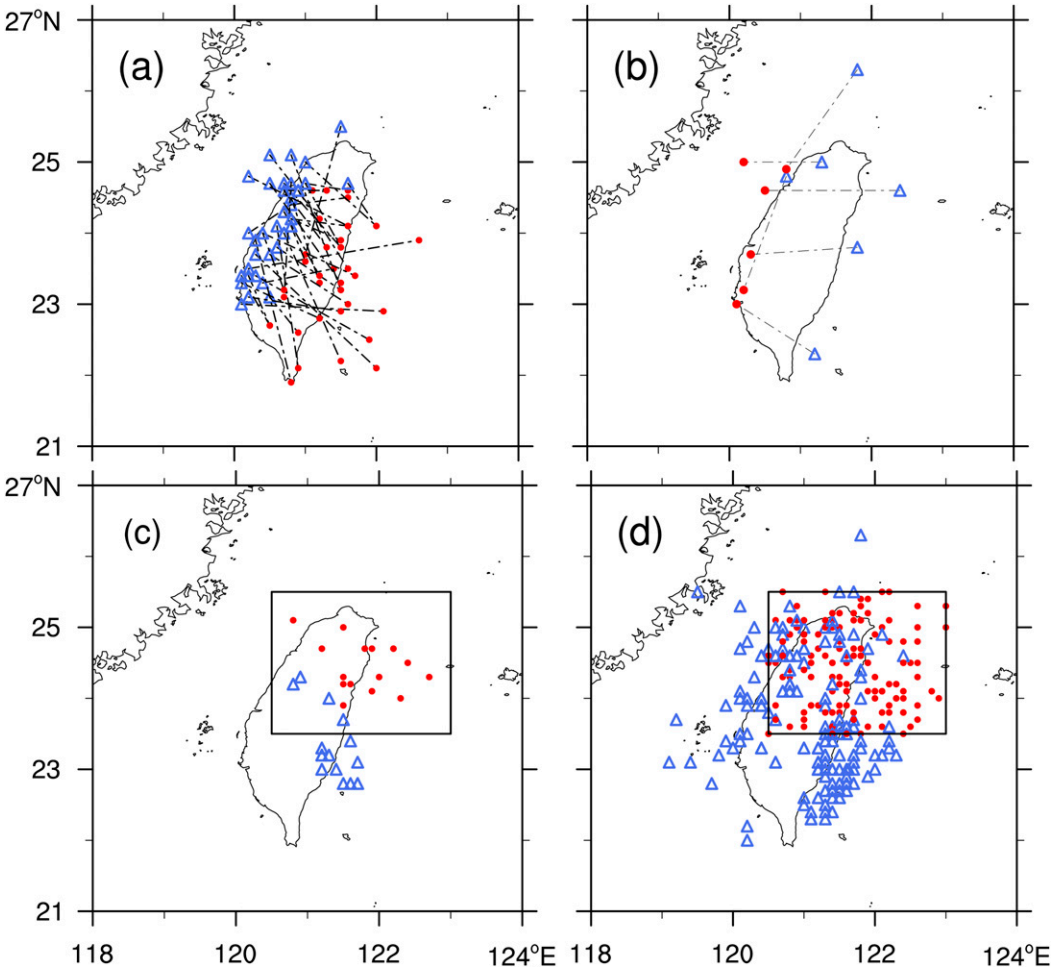

FIG. 7. Horizontal distribution of the discontinuous tracks of landfalling TCs (red dots) on the (a) east coast and (b) west coast of Taiwan Island. Also shown are landfalling TCs (c) with and (d) without looping movements over the inner box during the 66-yr period of 1949–2014. The corresponding SCs are represented by blue open triangles.

turn their looping tracks. Similar results have been found in the study of Typhoon Nari (2001) by Yang et al. (2008). In particular, their sensitivity simulations show the generation of looping tracks for Typhoon Nari, with its original vortex center replaced by an SC on the southern lee side when the CMR's height is systematically reduced (i.e., from 25% to 75%). The model-simulated secondary low and looping track are absent when the CMR is totally removed, however.

5. Summary and concluding remarks

In this study, the anomalous track changes of TCs as they move around Taiwan Island during the 66-yr period of 1949–2014 are statistically examined using the JTWC best-track data and mesoscale surface charts from the CWB Typhoon Data Base to help to improve our understanding and prediction of TC track changes over the WNP. Our major findings may be summarized as follows:

- A total of 530 TCs hit the target area covering Taiwan Island, with over 10% of them deflected more to the right than to the left when moving around Taiwan Island. The former were more distributed over Taiwan's northwestern coastal area, whereas the latter were more distributed over its eastern coast and the southern Taiwan Strait. In general, anomalous deflections of TCs were prone to occur over the northeast of Taiwan Island and the southern Taiwan Strait.
- Pronounced changes in TC translation speed were observed, with anomalous acceleration along Taiwan's eastern coast and anomalous deceleration over the southern Taiwan Strait.
- About 33% of the total TCs of interest, mostly from the STS to STY categories, were found to accompany

SCs, whose intensity ranged from 964 to 1008 hPa. The separation distance between the paired TCs and SCs varied from 33 to 643 km, with an average distance of 258 km. Results indicate that a stronger (weaker) SC was likely to occur when a stronger (weaker) TC approached the CMR with a shorter (longer) separation distance.

- Taiwan's NW quadrant had the most frequent formations of SCs, accounting for 38% of the total, followed by the SE, SW, and NE quadrants accounting for 28.5%, 27%, and 6.5%, respectively. A large percentage of the paired TCs and SCs were located on the opposite sides of the CMR, with only a few of them occurring on the same side.
- A total of 44 TCs, which was about 36% of the total TCs accompanying SCs, experienced discontinuous tracks, 38 (6) of which were crossing the CMR westbound (eastbound) and then were replaced by the SCs on the CMR's other side. The TCs with discontinuous tracks had an average Froude number of 1.57, which was smaller than that of 1.91 associated with continuous-tracking TCs.
- Only a total of 12 TCs (i.e., about 2.3% of the TCs) had looping tracks through northern Taiwan Island and its northeastern coastal water, and 11 of them were found to be accompanied by SCs on their southern or western side.

From the above results, we may conclude that moderate–intense TCs will likely experience anomalous changes in both translation speed and direction, albeit to different degrees, and will induce SCs on the lee side of the CMR as they move across Taiwan Island. This work appears to have important implications for the improved understanding and prediction of TC track changes when moving close to high mountainous regions. It is clear that the dynamical impact of topography on TC track changes is complicated partly because of multiscale interactions from large-scale flows to TC inner-core dynamics and latent heating and partly because of the TC location relative to the CMR as well as TC intensity. More case studies are needed to examine the roles of these different processes in determining the anomalous changes in both translation speed and direction by using a more dense observation dataset. Moreover, more detailed analyses and modeling studies need to be performed to gain insight into the formation of topographically induced SCs as TCs move across the CMR and the subsequent replacement of the corresponding original TC centers by the SCs.

Acknowledgments. We thank three anonymous reviewers for their critical comments that helped to improve the presentation of our results. This work was funded by the National Basic Research Program of China (973 Programs: 2015CB452804 and 2014CB441402); National Natural Science Foundation of China Grants 41475055, 41275093, 41475061, and 51778617; U.S. Office of Navy Research Grants N000141410143 and N000141712210; and NOAA Grant NA15NWS4680017.

REFERENCES

Bender, M. A., R. E. Tuleya, and Y. Kurihara, 1987: A numerical study of the effect of island terrain on tropical cyclones. *Mon. Wea. Rev.*, **115**, 130–155, https://doi.org/10.1175/1520-0493(1987)115<0130:ANSOTE>2.0.CO;2.

Brand, S., and J. W. Blelloch, 1974: Changes in the characteristics of typhoons crossing the island of Taiwan. *Mon. Wea. Rev.*, **102**, 708–713, https://doi.org/10.1175/1520-0493(1974)102<0708:CITCOT>2.0.CO;2.

Carr, L. E., III, and R. L. Elsberry, 1995: Monsoonal interactions leading to sudden tropical cyclone track changes. *Mon. Wea. Rev.*, **123**, 265–289, https://doi.org/10.1175/1520-0493(1995)123<0265:MILTST>2.0.CO;2.

Chan, J. C. L., W. M. Gray, and S. Q. Kidder, 1980: Forecasting tropical cyclone turning motion from surrounding wind and temperature fields. *Mon. Wea. Rev.*, **108**, 778–792, https://doi.org/10.1175/1520-0493(1980)108<0778:FTCTMF>2.0.CO;2.

——, F. M. F. Ko, and Y. M. Lei, 2002: Relationship between potential vorticity tendency and tropical cyclone motion. *J. Atmos. Sci.*, **59**, 1317–1336. https://doi.org/10.1175/1520-0469(2002)059<1317:RBPVTA>2.0.CO;2.

Chang, S. W.-J., 1982: The orographic effects induced by an island mountain range on propagating tropical cyclones. *Mon. Wea. Rev.*, **110**, 1255–1270, https://doi.org/10.1175/1520-0493(1982)110<1255:TOEIBA>2.0.CO;2.

Chen, L. S., and Y. H. Ding, 1979: *An Introduction to Typhoons over the Western North Pacific* (in Chinese). Science Press, 491 pp.

Dai, G. J., Y. R. Wen, and Y. Li, 2014: Statistical characteristics of tropical cyclone motion and sharp turning over northwestern Pacific (in Chinese). *J. Trop. Meteor.*, **30**, 23–33.

Hodanish, S., and W. M. Gray, 1993: An observational analysis of tropical cyclone recurvature. *Mon. Wea. Rev.*, **121**, 2665–2689, https://doi.org/10.1175/1520-0493(1993)121<2665:AOAOTC>2.0.CO;2.

Hsu, L.-H., H.-C. Kuo, and R. G. Fovell, 2013: On the geographic asymmetry of typhoon translation speed across the mountainous island of Taiwan. *J. Atmos. Sci.*, **70**, 1006–1022, https://doi.org/10.1175/JAS-D-12-0173.1.

Huang, J., J. Du, and W. Qian, 2015: A comparison between a generalized beta–advection model and a classical beta–advection model in predicting and understanding unusual typhoon tracks in eastern China seas. *Wea. Forecasting*, **30**, 771–792, https://doi.org/10.1175/WAF-D-14-00073.1.

Huang, Y.-H., C.-C. Wu, and Y. Wang, 2011: The influence of island topography on typhoon track deflection. *Mon. Wea. Rev.*, **139**, 1708–1727, https://doi.org/10.1175/2011MWR3560.1.

Jian, G.-J., and C.-C. Wu, 2008: A numerical study of the track deflection of Supertyphoon Haitang (2005) prior to its landfall in Taiwan. *Mon. Wea. Rev.*, **136**, 598–615, https://doi.org/10.1175/2007MWR2134.1.

Lin, Y.-L., and L. C. Savage III, 2011: Effects of landfall location and the approach angle of a cyclone vortex encountering a mesoscale mountain range. *J. Atmos. Sci.*, **68**, 2095–2106, https://doi.org/10.1175/2011JAS3720.1.

——, D. B. Ensley, S. Chiao, and C.-Y. Huang, 2002: Orographic influences on rainfall and track deflection associated with the passage of a tropical cyclone. *Mon. Wea. Rev.*, **130**, 2929–2950, https://doi.org/10.1175/1520-0493(2002)130<2929:OIORAT>2.0.CO;2.

——, S.-Y. Chen, C. M. Hill, and C.-Y. Huang, 2005: Control parameters for the influence of a mesoscale mountain range on cyclone track continuity and deflection. *J. Atmos. Sci.*, **62**, 1849–1866, https://doi.org/10.1175/JAS3439.1.

——, S.-H. Chen, and L. Liu, 2016: Orographic influence on basic flow and cyclone circulation and their impacts on track deflection of an idealized tropical cyclone. *J. Atmos. Sci.*, **73**, 3951–3974, https://doi.org/10.1175/JAS-D-15-0252.1.

Luo, Z.-X., and L.-S. Chen, 1995: Effect of orography of Taiwan Island on typhoon tracks (in Chinese). *Chin. J. Atmos. Sci.*, **19**, 701–706.

Meng, Z.-Y., X.-D. Xu, and L.-S. Chen, 1998: Mechanism of the impact of the cyclone system induced by the Taiwan Island topography on tropical cyclone unusual motion (in Chinese). *Chin. J. Atmos. Sci.*, **22**, 156–168.

Peng, L., S.-T. Wang, S.-L. Shieh, M.-D. Cheng, and T.-C. Yeh, 2012: Surface track discontinuity of tropical cyclones crossing Taiwan: A statistical study. *Mon. Wea. Rev.*, **140**, 121–139, https://doi.org/10.1175/MWR-D-10-05050.1.

Qian, C.-H., F.-Q. Zhang, B. W. Green, J. Zhang, and X.-Q. Zhou, 2013: Probabilistic evaluation of the dynamics and prediction of Supertyphoon Megi (2010). *Wea. Forecasting*, **28**, 1562–1577, https://doi.org/10.1175/WAF-D-12-00121.1.

Rappaport, E. N., and Coauthors, 2009: Advances and challenges at the National Hurricane Center. *Wea. Forecasting*, **24**, 395–419, https://doi.org/10.1175/2008WAF2222128.1.

Rostom, R., and Y.-L. Lin, 2015: Control parameters for track continuity of cyclones passing over the south-central Appalachian Mountains. *Wea. Forecasting*, **30**, 1429–1449, https://doi.org/10.1175/WAF-D-14-00080.1.

Shieh, S.-L., S.-T. Wang, M.-D. Cheng, and T.-C. Yeh, 1998: Tropical cyclone tracks over Taiwan from 1897 to 1996 and their applications (in Chinese). Central Weather Bureau Research Rep. CWB86-1M-01, 497 pp.

Tang, C. K., and J. C. L. Chan, 2014: Idealized simulations of the effect of Taiwan and Philippines topographies on tropical cyclone tracks. *Quart. J. Roy. Meteor. Soc.*, **140**, 1578–1589, https://doi.org/10.1002/qj.2240.

——, and ——, 2015: Idealized simulations of the effect of local and remote topographies on tropical cyclone tracks. *Quart. J. Roy. Meteor. Soc.*, **141**, 2045–2056, https://doi.org/10.1002/qj.2498.

Wang, C.-C., Y.-H. Chen, H.-C. Kuo, and S.-Y. Huang, 2013: Sensitivity of typhoon track to asymmetric latent heating/rainfall induced by Taiwan topography: A numerical study of Typhoon Fanapi (2010). *J. Geophys. Res Atmos.*, **118**, 3292–3308, https://doi.org/10.1002/jgrd.50351.

Wang, S.-T., 1954: A study on typhoons crossing the Central Mountain Range of Taiwan (in Chinese). *Chin. Wea. Anal. Mon.*, **4**, 10–30.

——, 1980: Prediction of the movement and strength of typhoons in Taiwan and its vicinity (in Chinese). National Science Council Research Rep. 108, 100 pp.

Wu, C.-C., 2001: Numerical simulation of Typhoon Gladys (1994) and its interaction with Taiwan terrain using the GFDL hurricane model. *Mon. Wea. Rev.*, **129**, 1533–1549, https://doi.org/10.1175/1520-0493(2001)129<1533:NSOTGA>2.0.CO;2.

——, and Y.-H. Kuo, 1999: Typhoons affecting Taiwan: Current understanding and future challenges. *Bull. Amer. Meteor. Soc.*, **80**, 67–80, https://doi.org/10.1175/1520-0477(1999)080<0067:TATCUA>2.0.CO;2.

——, T.-H. Li, and Y.-H. Huang, 2015: Influence of mesoscale topography on tropical cyclone tracks: Further examination of the channeling effect. *J. Atmos. Sci.*, **72**, 3032–3050, https://doi.org/10.1175/JAS-D-14-0168.1.

Wu, L., H. Zong, and J. Liang, 2011: Observational analysis of sudden tropical cyclone track changes in the vicinity of the East China Sea. *J. Atmos. Sci.*, **68**, 3012–3031, https://doi.org/10.1175/2010JAS3559.1.

——, Z. Ni, J. Duan, and H. Zong, 2013: Sudden tropical cyclone track changes over the western North Pacific: A composite study. *Mon. Wea. Rev.*, **141**, 2597–2610, https://doi.org/10.1175/MWR-D-12-00224.1.

Xie, B., and F. Zhang, 2012: Impacts of typhoon track and island topography on the heavy rainfalls in Taiwan associated with Morakot (2009). *Mon. Wea. Rev.*, **140**, 3379–3394, https://doi.org/10.1175/MWR-D-11-00240.1.

Yang, M.-J., D.-L. Zhang, and H.-L. Huang, 2008: A modeling study of Typhoon Nari (2001) at landfall. Part I: Topographic effects. *J. Atmos. Sci.*, **65**, 3095–3115, https://doi.org/10.1175/2008JAS2453.1.

——, ——, X.-D. Tang, and Y. Zhang, 2011: A modeling study of Typhoon Nari (2001) at landfall: 2. Structural changes and terrain-induced asymmetries. *J. Geophys. Res.*, **116**, D09112, https://doi.org/10.1029/2010JD015445.

Yeh, T.-C., and R. L. Elsberry, 1993a: Interaction of typhoons with the Taiwan orography. Part I: Upstream track deflections. *Mon. Wea. Rev.*, **121**, 3193–3212, https://doi.org/10.1175/1520-0493(1993)121<3193:IOTWTT>2.0.CO;2.

——, and ——, 1993b: Interaction of typhoons with the Taiwan topography. Part II: Continuous and discontinuous tracks across the island. *Mon. Wea. Rev.*, **121**, 3213–3233, https://doi.org/10.1175/1520-0493(1993)121<3213:IOTWTT>2.0.CO;2.

Zhang, X., Y. Li, D.-L. Zhang, and L. Chen, 2018: A 65-yr climatology of unusual tracks of tropical cyclones in the vicinity of China's coastal waters during 1949–2013. *J. Appl. Meteor. Climatol.*, **57**, 155–170, https://doi.org/10.1175/JAMC-D-16-0392.1.